Eur. Phys. J. C (2014) 74:2785
DOI 10.1140/epjc/s10052-014-2785-7

THE EUROPEAN PHYSICAL JOURNAL C

Regular Article - Theoretical Physics

Tsallis statistics approach to the transverse momentum distributions in p–p collisions

Maciej Rybczyński[a], **Zbigniew Włodarczyk**[b]

Institute of Physics, Jan Kochanowski University, ul. Swietokrzyska 15, 25406 Kielce, Poland

Received: 23 January 2014 / Accepted: 14 February 2014 / Published online: 26 February 2014

Abstract Transverse momentum distributions of negatively charged pions produced in p–p interactions at beam momenta 20, 31, 40, 80, and 158 GeV/c are studied using the Tsallis distribution as a parametrization. Results are compared with higher energy data and changes of parameters with energy are determined. Different Tsallis-like distributions are compared.

1 Introduction

Transverse momentum (p_{T}) distributions of identified hadrons are the most common tools used to study the dynamics of high energy collisions. The p–p interactions are used as a baseline and are important to understand the particle production mechanism [1]. In the framework of Tsallis statistics [2–5] the momentum distribution is given by

$$\frac{\mathrm{d}^3 N}{\mathrm{d}p^3} = \frac{gV}{(2\pi)^3}\left[1+(q-1)\frac{E-\mu}{T}\right]^{\frac{q}{1-q}} \xrightarrow{q\to 1} \frac{gV}{(2\pi)^3}\exp\left(-\frac{E-\mu}{T}\right), \qquad (1)$$

where T and μ are the temperature and the chemical potential, V is the volume, and g is the degeneracy factor. In this form, Eq. (1) is usually supposed to represent a nonextensive generalization of the Boltzmann–Gibbs exponential distribution, $\exp(-E/T)$, with q being a new parameter, in addition to the previous 'temperature' T. Such an approach is known as nonextensive statistics [2,3], in which the parameter q summarily describes all features causing a departure from the usual Boltzmann–Gibbs statistics. In particular it was shown in [6] that $q-1 = \mathrm{Var}(T)/\langle T\rangle^2$ and this directly describes intrinsic fluctuations of the temperature (however, the Tsallis distribution also emerges from a number of other more dynamical mechanisms, for example see [7] for more details and references). This approach has been shown to be very successful in describing multiparticle production processes of a different kind (see [7–9] for recent reviews). In terms of transverse momentum, transverse mass, $m_{\mathrm{T}} = \sqrt{m^2+p_{\mathrm{T}}^2}$, and rapidity y, Eq. (1) becomes

$$\frac{\mathrm{d}^2 N}{p_{\mathrm{T}}\mathrm{d}p_{\mathrm{T}}\mathrm{d}y} = gV\frac{m_{\mathrm{T}}\cosh(y)}{(2\pi)^2} \times\left[1+(q-1)\frac{m_{\mathrm{T}}\cosh(y)-\mu}{T}\right]^{\frac{q}{1-q}}. \qquad (2)$$

It has been shown repeatedly that the Tsallis distribution gives an excellent description of p_{T} spectra measured in p–p collisions at RHIC ($\sqrt{s}=62.4$ and 200 GeV) and LHC ($\sqrt{s} = 0.9, 2.76$, and 7.0 TeV) energies [4,10–13]. In particular, changes in the transverse momentum distribution with energy (using data at energies 0.54, 0.9, 2.36, and 7 TeV) are studied using the Tsallis distribution (2) as a parametrization [14]. In this paper we extend this analysis to transverse momentum spectra obtained in p–p collisions at $\sqrt{s}=6.27, 7.74, 8.76, 12.32$, and 17.27 GeV by the NA61/SHINE Collaboration [15].[1] In addition to the possibility of studying collisions at low incident energies, the measurements performed by NA61/SHINE Collaboration allow us to study the low-p_{T} part of the spectra. The values of T and V are very sensitive to the low-p_{T} part of the transverse momentum distribution, and extending the analysis to lower p_{T} could bring much clarification here.

[a] e-mail: Maciej.Rybczynski@ujk.edu.pl

[b] e-mail: Zbigniew.Wlodarczyk@ujk.edu.pl

[1] Recently, the experimental results on inclusive spectra of negatively charged pions produced in inelastic p–p interactions at beam momenta 20, 31, 40, 80, and 158 GeV/c were presented [15]. The measurements were performed using the large acceptance NA61/SHINE hadron spectrometer at the CERN Super Proton Synchrotron. Numerical results corresponding to the two dimensional spectra in transverse momentum and rapidity corrected for experimental biases were given in Ref. [16].

2 Analysis of transverse momentum distributions

Transverse momentum spectra of negatively charged pions are fitted using the Tsallis distribution given by Eq. (2) with $g_{\pi^-} = 1$ and $\mu = 0$. It is worth to be noted that the variable T and V are functions of μ at fixed values of q,

$$T = T_0 + (q-1)\mu, \tag{3}$$

$$V = V_0[1+(q-1)\mu/T_0]^{q/(1-q)} = V_0(T/T_0)^{q/(1-q)}, \tag{4}$$

and they can be calculated if the parameters $T = T_0$ and $V = V_0$ at $\mu = 0$ are known [14].

The Tsallis distribution describes the transverse momentum distributions of negatively charged pions in p–p collisions as obtained by the NA61/SHINE Collaboration [15] in all rapidity intervals remarkably well as shown in Fig. 1. The values of the nonextensivity parameters q needed to describe the transverse momentum distributions of negatively charged pions are shown in Fig. 2. The values of the temperature parameter T for different energies and rapidity intervals are shown in Fig. 3. The temperature parameter T shows a clear rapidity dependence, which we have parametrized as $T \simeq 0.09\cosh(y)$.

3 Energy dependence of parameters

The energy dependence of the various parameters is displayed in Figs. 4, 5, and 6. For comparison with higher energy data [14], which are for mid-rapidity $y = 0$, we show the parameters as evaluated for rapidity interval $0 < y < 0.2$. All analyzed parameters show a clear but weak energy dependence, which we have parametrized as

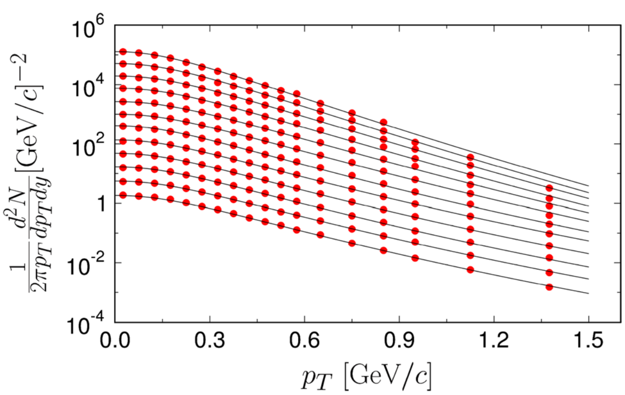

Fig. 1 (Color online) Transverse momentum distributions of negatively charged pions produced in p–p collisions as obtained by the NA61/SHINE Collaboration [15] at $\sqrt{s} = 17.27$ GeV in rapidity intervals $0.2k < y < 0.2(k+1)$ where $k = 0, \ldots, 11$ from the bottom up. Data points for different rapidity bins were scaled by 3^k for better readability

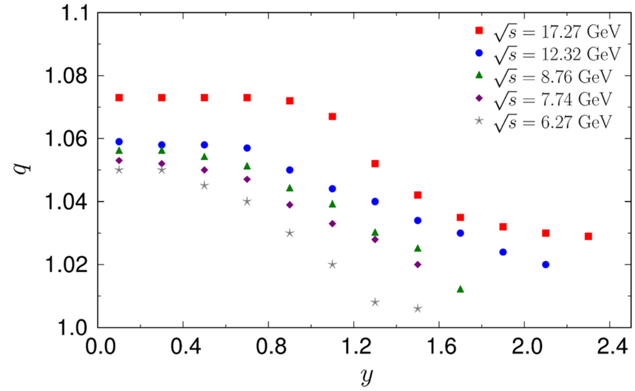

Fig. 2 (Color online) The values of the nonextensivity parameter q, as a function of rapidity obtained from fits to the transverse momentum distributions at different energies

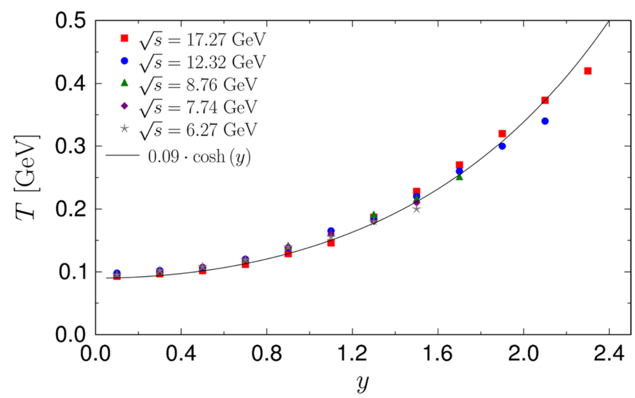

Fig. 3 (Color online) The values of the temperature parameter, T, as a function of rapidity obtained from fits to the transverse momentum distributions at different energies

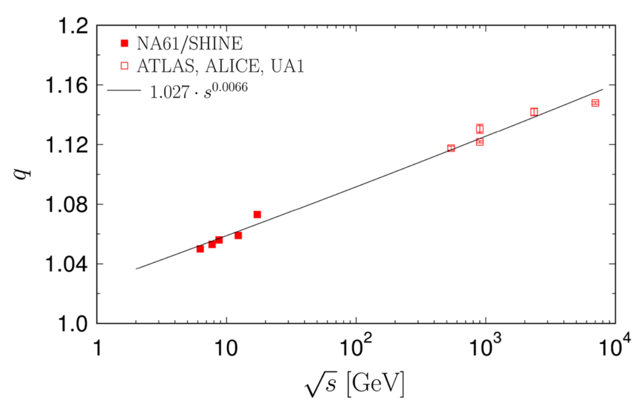

Fig. 4 (Color online) Energy dependence of the parameter q appearing in the Tsallis distribution. *Open points* are from ATLAS, ALICE, and UA1 Collaborations data (taken from Ref. [14]). *Solid points* are from NA61/SHINE Collaboration data [15]. Data are fitted by Eq. (5)

$$q(s) = 1.027(\sqrt{s})^{0.01326}, \tag{5}$$

$$T(s) = 0.1014(\sqrt{s})^{-0.03262}, \tag{6}$$

$$R(s) = \left(\frac{3V(s)}{4\pi}\right)^{1/3} = 2.31(\sqrt{s})^{0.09}. \tag{7}$$

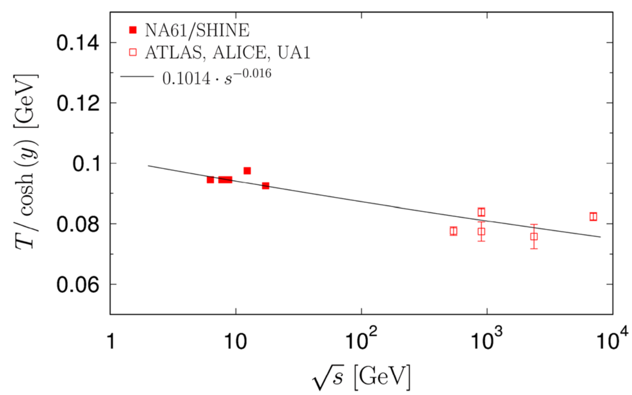

Fig. 5 (Color online) Energy dependence of the temperature parameter T appearing in the Tsallis distribution. *Open points* are from ATLAS, ALICE, and UA1 Collaborations data (taken from Ref. [14]). *Solid points* are from NA61/SHINE Collaboration data [15]. Data are fitted by Eq. (6)

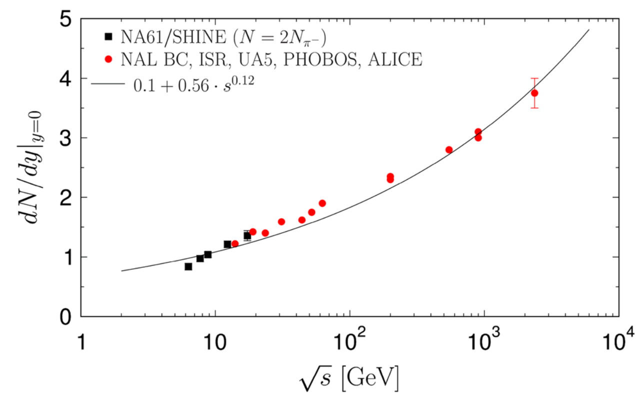

Fig. 7 (Color online) dN/dy of charged particles produced in the central rapidity region as a function of the center-of mass energy in p–p and p–p̄ collisions. The energy dependence given by Eq. (9) is compared with inelastic measurements from NA61/SHINE [15] (p–p), NAL Bubble Chamber (p–p̄), ISR (p–p), UA5 (p–p̄), PHOBOS (p–p), and ALICE (p–p) experiments taken from the compilation [19]

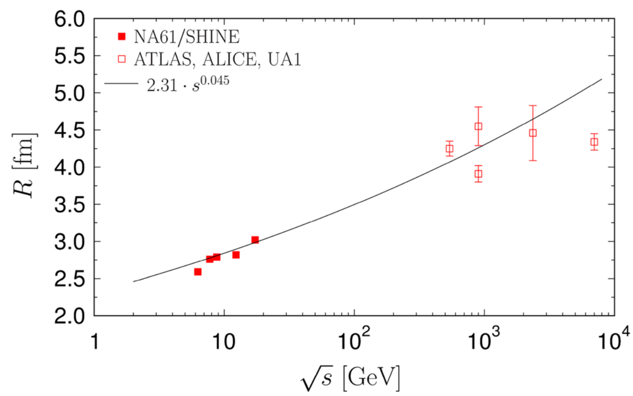

Fig. 6 (Color online) Energy dependence of the radius R appearing in the volume factor, $V = 4/3\pi R^3$. *Open points* are from ATLAS, ALICE, and UA1 Collaborations data (taken from Ref. [14]). *Solid points* are from NA61/SHINE Collaboration data [15]. Data are fitted by Eq. (7)

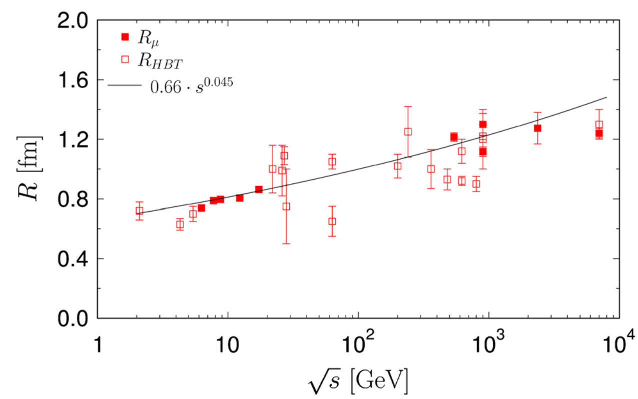

Fig. 8 (Color online) Energy dependence of the radius $R_\mu = R_{\mu=0}/3.5$ (*solid points*) in comparison with HBT measurements of source radii obtained in hadron–hadron reactions [20] (*open points*)

The value of R is not necessarily related to the size of the system as deduced from a HBT analysis [17,18] but serves to fix the normalization of the distribution (2). In particular, we have

$$\left.\frac{\mathrm{d}N}{\mathrm{d}y}\right|_{y=0} = \frac{gVT}{(2\pi)^2}\left[1+(q-1)\frac{m}{T}\right]^{\frac{1}{1-q}} \times \frac{(2-q)m^2+2mT+2T^2}{(2-q)(3-2q)}. \quad (8)$$

For the energy dependence of parameters $q(s)$, $T(s)$, and $R(s)$, evaluated above, given by Eqs. (5–7) we have

$$\left.\frac{\mathrm{d}N}{\mathrm{d}y}\right|_{y=0} \simeq 0.1 + 0.56(\sqrt{s})^{0.24}. \quad (9)$$

The energy dependence of dN/dy in the central rapidity region in comparison with inelastic measurements is shown in Fig. 7.

We can treat the size of the system, R, more thoroughly. The radius given by Eq. (7) is calculated for $\mu = 0$. For other values of the chemical potential, the size is smaller (cf. Eqs. (3) and (4)). Comparing $R(s)$ with the experimental data deduced from the HBT analysis we see that $R_{HBT} \simeq R/\kappa$, where $\kappa = 3.5$. In Fig. 8 we display $R(s)/\kappa$ in comparison with data obtained from HBT analysis [20].

Following this observation we assume

$$V_{\mu=0} = V_\mu \cdot \kappa^3, \quad (10)$$

and from Eqs. (3) and (4) we have

$$\mu = \frac{T_{\mu=0}}{q-1}\left(\kappa^{3(q-1)/q} - 1\right) \quad (11)$$

and using parameterizations (5) and (6) we have an energy dependence of the chemical potential in the form

$$\mu(s) \simeq 0.39(\sqrt{s})^{-0.022}. \tag{12}$$

4 Different parameterizations

Almost 50 years ago Hagedorn developed a statistical description of momentum spectra observed in multiparticle production processes [21]. Hagedorn's approach predicts an exponential decay of the momentum distribution,

$$E\frac{d^3N}{dp^3} \simeq C\exp\left(-\frac{p_T}{T}\right), \tag{13}$$

for transverse momenta, whereas in experiment one observes a non-exponential behavior for large transverse momenta. Subsequently, Hagedorn proposed the 'QCD inspired' empirical formula describing the data of the invariant momentum distribution of hadrons as a function of p_T over a wide range [22]:

$$E\frac{d^3N}{dp^3} = C\left(1+\frac{p_T}{p_0}\right)^{-n} \rightarrow \begin{cases} \exp(-np_T/p_0) & \text{for } p_T \rightarrow 0, \\ (p_T/p_0)^{-n} & \text{for } p_T \rightarrow \infty, \end{cases} \tag{14}$$

with C, p_0, and n being fit parameters. This becomes a pure exponential for small p_T and a pure power law for large p_T. For $n = q/(q-1)$ and $p_0 = T/(q-1)$, the Hagedorn formula (14) coincides with the Tsallis distribution [2,3],

$$E\frac{d^3N}{dp^3} = C\left[1-(1-q)\frac{p_T}{T}\right]^{\frac{q}{1-q}}. \tag{15}$$

The basic conceptual difference between (14) and (15) is in the underlying physical picture. In (14) the low-p_T region is controlled by soft physics represented by some unknown unperturbative theory or model, and the high-p_T region is governed by hard physics represented by perturbative QCD. In (15), the nonextensive formula works in the whole range of p_T and it is not derived from some particular theory. It is only a generalization of the regular statistical mechanics and just offers the kind of universal unifying principle, namely the existence of some kind of equilibrium affecting all scales of p_T, which is described by two parameters, T and q. The temperature T characterize its mean properties and the parameter q, known as the nonextensivity parameter, expresses action of the potentially non-trivial long range effects believed to be caused by fluctuations [6] (but also by some correlations or long memory effects [2,3]). It is worth to be noted that the invariant momentum distribution in the form (cf. Eq. (1))

$$E\frac{d^3N}{dp^3} = \frac{gV}{(2\pi)^3}\left[1+(q-1)\frac{E}{T}\right]^{\frac{q}{1-q}}, \tag{16}$$

results in Eq. (2) without pre-factor $m_T\cosh(y)$ on the right hand side of the equation. For the non-relativistic energies ($E = p^2/(2m)$), Eq. (16) corresponds to the Tsallis distribution

$$E\frac{d^3N}{dp^3} = \frac{gV}{(2\pi)^3}\left[1+(q-1)\frac{p^2}{2mT}\right]^{\frac{q}{1-q}}, \tag{17}$$

originating from multiplicative noise [23,24].[2]

The exponential function Eq. (13) describes data only in a limited range of transverse momentum, $0.15 < p_T < 0.6$ [15]. As shown in Fig. 1, the Tsallis distribution given by Eq. (2) describes the whole p_T range remarkably well.

All Tsallis-like distributions lead to a power-law tail,

$$\frac{d^2N}{p_T dp_T dy} \propto p_T^{-n}, \tag{18}$$

of the distribution for sufficiently large transverse momenta. The difference between them can be seen in the low p_T region, where

$$\frac{d^2N}{p_T dp_T dy} \propto \begin{cases} \alpha - \beta p_T + \gamma p_T^2 & \text{for Eqs. (13), (14), (15)} \\ \alpha - \gamma p_T^2 & \text{for Eqs. (1), (16), (17)} \end{cases} \tag{19}$$

The parameters α, β, and γ are positive valued functions of q and T (in the case of Eq. (1), $T < m$ is required for $\gamma > 0$). In the low p_T region, Tsallis-like distributions with variable p_T^2 differs from the one expressed in variable p_T. A comparison of different parameterizations is shown in Fig. 9.

5 Discussion and conclusions

In conclusion, the Tsallis distribution, Eq. (2), leads to an excellent description of the data on the transverse momentum. By comparing results from NA61/SHINE [15] with the results obtained at higher energies [14] it has been possible to extract the energy dependence of the parameters q, T, and R. A consistent picture emerges from a comparison of the fits using the Tsallis distribution in a wide range of energies.

[2] The Langevin equation $dp/dt + \gamma(t)p = \xi(t)$ leads to a power-law tail of the distribution for sufficiently large momenta. Here both $\gamma(t)$ and $\xi(t)$ denote stochastic processes (traditional multiplicative noise and additive noise, respectively). As shown in [23] in the case of $\mathrm{Cov}(\gamma, \xi) = 0$ and $E(\xi) = 0$ (i.e., for, respectively, no correlation between the noises and no drift term due to the additive noise) the solution is given by the non-normalized Tsallis distribution for the variable p^2.

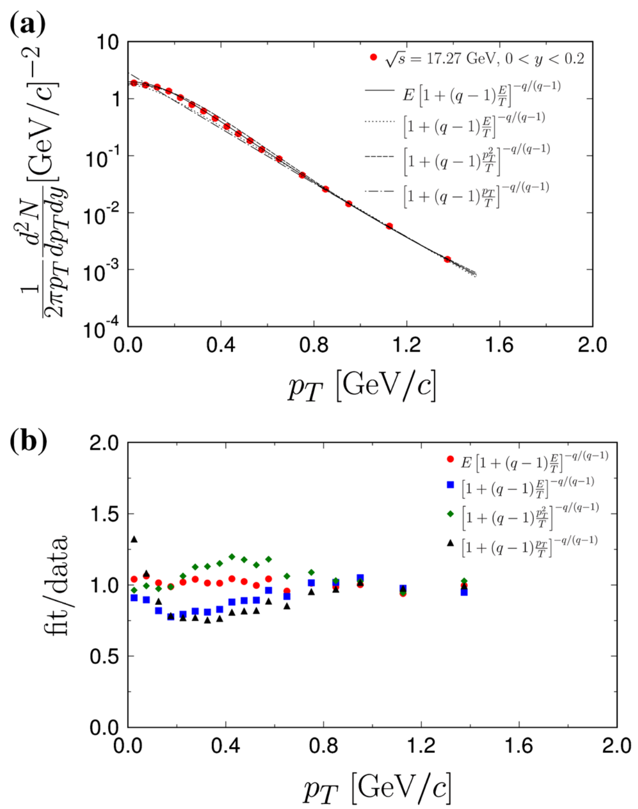

Fig. 9 (Color online) **a** Transverse momentum distribution of negatively charged pions produced in p–p collisions at $\sqrt{s} = 17.27$ GeV in the rapidity interval $0 < y < 0.2$ [15] fitted by different parameterizations (with normalization at the high p_T region). **b** Ratio fit/data for the results presented in (**a**)

Different parameterizations lead not only to different qualities of the fits but also to different values of the parameters. In Ref. [15] experimental data are fitted by an exponential distribution (13) in a limited range of the transverse momenta ($0.15 < p_T < 0.6$ GeV/c) on evaluating the temperature parameters, seemingly larger than our estimate based on the parametrization (2). Such a difference in the values of the temperature parameters is fully understandable. For distributions with the same mean transverse momentum, $\langle p_T \rangle$, the parameter T_{exp} evaluated from Eq. (13) is connected with the parameter T evaluated from Eq. (2) by the relation

$$T_{exp} \simeq a + b \cdot T, \tag{20}$$

where, numerically, $a = 0.31 - 0.654q + 0.354q^2$ and $b = 27.35 - 55q + 29.07q^2$. Moreover, it is remarkable that the parametrization (1) proposed by Cleymans [4,5] is for the momentum distribution, d^3N/dp^3, while the other Tsallis-like parameterizations (14)–(17) are for the invariant distribution, Ed^3N/dp^3.

Acknowledgments This research was supported by the National Science Center (NCN) under contracts: 2011/03/B/ST2/02617 and 2012/04/M/ST2/00816.

References

1. F. Becattini, U.W. Heinz, Z. Phys, C 76, 269 (1997). [Erratum-ibid. C 76, 578 (1997)]. [hep-ph/9702274]
2. C. Tsallis, J. Statist. Phys. **52**, 479 (1988)
3. C. Tsallis, Eur. Phys. J. A **40**, 257 (2009). [arXiv:0812.4370 [physics.data-an]] and Introduction to Nonextensive Statistical Mechanics (Springer, 2009). For an updated bibliography on this subject, see http://tsallis.cat.cbpf.br/biblio.htm
4. J. Cleymans, D. Worku, J. Phys. G **39**, 025006 (2012). [arXiv:1110.5526[hep-ph]]
5. J. Cleymans, D. Worku, Eur. Phys. J. A **48**, 160 (2012). [arXiv:1203.4343[hep-ph]]
6. G. Wilk, Z. Wlodarczyk, Phys. Rev. Lett. **84**, 2770 (2000). [hep-ph/9908459]
7. G. Wilk, Z. Wlodarczyk, Eur. Phys. J. A **48**, 161 (2012). [arXiv:1203.4452 [hep-ph]]
8. G. Wilk, Z. Wlodarczyk, Eur. Phys. J. A **40**, 299 (2009). [arXiv:0810.2939 [hep-ph]]
9. G. Wilk, Z. Wlodarczyk, Central. Eur. J. Phys. **10**, 568 (2012). [arXiv:1110.4220 [hep-ph]]
10. I. Sena, A. Deppman, Eur. Phys. J. A **49**, 17 (2013). [arXiv:1209.2367 [hep-ex]].
11. A. Adare et al. [PHENIX Collaboration], Phys. Rev. D **83**, 052004 (2011) [arXiv:1005.3674 [hep-ex]]
12. P.K. Khandai, P. Sett, P. Shukla, V. Singh, Int. J. Mod. Phys. A **28**, 1350066 (2013). [arXiv:1304.6224 [hep-ph]]
13. C.-Y. Wong, G. Wilk, Acta Phys. Polon. B **43**, 2047 (2012). [arXiv:1210.3661 [hep-ph]]
14. J. Cleymans, G.I. Lykasov, A.S. Parvan, A.S. Sorin, O.V. Teryaev, D. Worku, Phys. Lett. B **723**, 351 (2013). [arXiv:1302.1970 [hep-ph]]
15. N. Abgrall et al. [NA61/SHINE Collaboration], Eur. Phys. J. C. [arXiv:1310.2417 [hep-ex]]
16. for numerical data, see https://edms.cern.ch/document/1314605
17. K. Aamodt et al. [ALICE Collaboration], Phys. Rev. D **82**, 052001 (2010). [arXiv:1007.0516 [hep-ex]]
18. M.M. Aggarwal et al. [STAR Collaboration], Phys. Rev. C **83**, 064905 (2011). [arXiv:1004.0925 [nucl-ex]]
19. V. Khachatryan et al. [CMS Collaboration], Phys. Rev. Lett. **105**, 022002 (2010). [arXiv:1005.3299 [hep-ex]]
20. T. Kageya, Bose–Einstein correlation from pions produced in pp collisions, in *Correlations and Multiparticle Production*, ed. by M. Plumer, S. Raha, R. Weiner (World Scientific, Singapore, 1991)
21. R. Hagedorn, Nuovo Cim. Suppl. **3**, 147 (1965)
22. R. Hagedorn, Riv. Nuovo Cim. **6N10**, 1 (1984)
23. T.S. Biro, A. Jakovac, Phys. Rev. Lett. **94**, 132302 (2005). [hep-ph/0405202]
24. C. Anteneodo, C. Tsallis, J. Math. Phys. **44**, 5194 (2003)